

Climate Change and the Middle Atmosphere. Part I: The Doubled CO₂ Climate

D. RIND

NASA Goddard Space Flight Center, Institute for Space Studies, New York

R. SUOZZO

Sigma Data Service Corporation, New York, New York

N. K. BALACHANDRAN

Lamont-Doherty Geological Observatory of Columbia University, Palisades, New York

M. J. PRATHER

NASA Goddard Space Flight Center, Institute for Space Studies, New York

(Manuscript received 14 October 1988, in final form 12 September 1989)

ABSTRACT

The impact of doubled atmospheric CO₂ on the climate of the middle atmosphere is investigated using the GISS global climate/middle atmosphere model. In the standard experiment, the CO₂ concentration is doubled both in the stratosphere and troposphere, and the sea surface temperatures are increased to match those of the doubled CO₂ run of the GISS 9 level climate model. Additional experiments are run to determine how the middle atmospheric effects are influenced by tropospheric changes, and to separate the dynamic and radiative influences. These include the use of the greater high latitude/low latitude surface warming ratio generated by the Geophysical Fluid Dynamics Laboratory doubled CO₂ experiments, doubling the CO₂ only in either the troposphere or stratosphere, and allowing the middle atmosphere to react only radiatively.

As expected, doubled CO₂ produces warmer temperatures in the troposphere, and generally cooler temperatures in the stratosphere. The net result is a decrease of static stability for the atmosphere as a whole. In addition, the 100 mb warming maximizes in the tropics, leading to improved propagation conditions for planetary waves, and increased potential energy in the lower stratosphere. These processes generate increased eddy energy in the middle atmosphere in most seasons. With greater eddy energy comes greater eddy forcing of the mean flow and an increase in the intensity of the residual circulation from the equator to the pole, which tends to warm high latitudes. Increased gravity wave drag in some of the experiments also helps to intensify the circulation. The middle atmosphere dynamical differences are on the order of 10%–20% of the model values for the current climate, and, along with the calculated temperature differences of up to some 10°C, may have a significant impact on the chemistry of the future atmosphere including that of stratospheric ozone, the polar ozone "hole," and basic atmospheric composition.

1. Introduction

By the middle of the next century, current projections indicate that the earth's climate will be significantly different from that of today, due to increasing concentrations in trace gases with greenhouse capacity. Given the current and expected growth in these gases, it is estimated that the equivalent doubled CO₂ radiative forcing will be achieved around 2040 (e.g., Ramanathan et al. 1985). With one such scenario for trace gas growth, Hansen et al. (1988) found that in the GISS 9-level global climate model (which is basically a tropospheric model, with only the lower stratosphere included in the dynamics), the surface air warming equivalent to that for doubled CO₂ would

occur about 2060 A.D. Increased radiative cooling in the stratosphere would accompany this tropospheric warming.

On the same time scale, anthropogenically generated chlorine may have a significant impact on ozone in the middle atmosphere (defined approximately as the region of 10–100 km in altitude). While such effects are currently thought to be involved in the Southern Hemisphere ozone hole phenomena and are just detectable in the Northern Hemisphere (NASA 1988), future changes in ozone may well be more severe, as the chlorine concentrations build up in the stratosphere. Various models have been used to project ozone changes into the middle of the next century (e.g., Brasseur et al. 1985; Isaksen and Stordal 1986; Connell and Wuebbles 1986), and while the actual assessments may well have to be altered if freon production decreases significantly, long-term changes in ozone are still likely (NASA 1988). The task of predicting the future atmosphere is complicated because changes in other gases

Corresponding author address: Dr. David Rind, Goddard Space Flight Center, Institute for Space Studies, 2880 Broadway, Room 7450, New York, NY 10025.

such as methane and water vapor are also likely to be occurring. In addition, the projected climate changes due to increased greenhouse effect have the potential to alter ozone change assessments.

Several studies have attempted to quantify the impact of changing climate on chlorine-induced ozone depletion, using 2-D stratospheric models (Wuebbles et al. 1983; Brasseur and De Rudder 1987; Ramathan et al. 1987). The results showed that the depletions are somewhat ameliorated by the projected changes in temperature. As indicated by Brasseur and Hitchman (1988), the stratospheric temperature change due to increased CO₂ will by itself affect ozone distributions. In those studies, other possible alterations of the middle atmosphere, such as changes in atmospheric transport, had to be ignored. This paper presents results from a 3-D model that show that the effect of changing climate on both middle atmosphere temperatures and dynamics will likely have an effect on ozone distributions.

Increasing levels of CO₂ should by themselves cool the stratosphere, due to an increased loss of longwave radiation to space. Labitzke et al. (1986) report that Northern Hemisphere temperature data at the 30 mb level for the last 20 years already depict a cooling, on the order of 0.24°C/decade for the hemisphere as a whole. This result is in excellent agreement with cooling that arises at that level in the GISS climate model, when run for the past 20 years with trace gases added in a realistic time-transgressive manner (Hansen et al. 1988). It has been estimated using both narrowband radiance models (Kiehl 1986), and the upper level radiation layers in the GISS climate model, that the additional radiative cooling due to doubled CO₂ would reduce upper stratospheric temperatures on the order of 10°C.

There have now been several well-publicized simulations of the effect of doubled CO₂ on tropospheric climate (e.g., Manabe and Wetherald 1975; Hansen et al. 1984; Washington and Mielh 1984; Manabe and Wetherald 1987; Wilson et al. 1987). The models show general agreement on the magnitude of the change in the global, annual average surface air temperature, with warming of 4°–5°C. While they exhibit individual differences, all the models show alterations of various tropospheric dynamical properties. Given the importance of planetary waves and gravity waves generated in the troposphere on the dynamics of the stratosphere, tropospheric changes must be taken into account in any assessment of the impact of doubled CO₂ on stratospheric circulation.

Much less work has been reported on the impact of doubled CO₂ climate changes on the middle atmosphere. Fels et al. (1980) investigated the sensitivity of the stratosphere to various radiative perturbations, including doubled CO₂. The results were strongly constrained by keeping the sea surface temperatures at present-day values, thereby limiting the possible influence of the tropospheric response. In addition, annual

mean conditions were used. Boville (1986) doubled the CO₂ in a perpetual January experiment but again minimizing its tropospheric effect by keeping sea surface temperatures fixed at current values. As was recognized in both studies, the problem has not been considered in its entirety.

In this paper we investigate the full impact of the doubled CO₂ climate change on the middle atmosphere. We report on a number of experiments that show that tropospheric changes play an important role in altering the dynamics of the doubled CO₂ middle atmosphere. This is the first of a series of studies investigating the impact of climate change on the middle atmosphere.

2. Model and experiments

The model used for these experiments is the GISS Global Climate Middle Atmosphere Model (GCMAM) (Rind et al. 1988a,b; henceforth I and II). The model has 8° × 10° (latitude by longitude) resolution, extends from the surface to 85 km, and includes all the processes used in the GISS climate model (Hansen et al. 1983) (e.g., numerical solutions of the primitive equations, calculation of radiative and surface fluxes, a complete hydrologic cycle with convective and cloud parameterizations, etc.). In addition, it incorporates a parameterization for gravity wave generation, propagation, breaking and drag, based on linear saturation theory, with all the parameters evaluated as a function of model-generated wind and temperature fields (I). The GCMAM produces a generally realistic simulation of the troposphere and middle atmosphere, for both the mean fields and variability (I, II). Its primary deficiencies are somewhat reduced longwave energy in the lower stratosphere, too cold temperatures near the model top, and too warm temperatures in the Southern Hemisphere polar lower stratosphere.

To investigate the response of the middle atmosphere to the doubled CO₂ climate, we first doubled the CO₂ (from 315 to 630 ppm) throughout the atmosphere and incorporated the boundary conditions generated when CO₂ was doubled in the GISS 9-level climate model (Hansen et al. 1984). The 9-level model was run to equilibrium allowing the sea surface temperatures to change, and produced an average warming of 4.2°C. Included in the boundary condition specifications for the middle atmosphere model experiment were the altered sea surface temperatures, as well as altered ground hydrologic conditions and sea ice. We thus enable the middle atmosphere model to react to changes in tropospheric dynamics [as discussed, for example, in Rind (1986, 1988)] and warming without running the model to equilibrium. As this experiment incorporates the standard conditions for doubled CO₂ in the GISS model it will be referred to as "2CO₂."

To investigate why the middle atmosphere was changing, and how sensitive the results were to tro-

ospheric specifications, a number of additional experiments were performed. In one experiment we limited the tropospheric response by specifying the sea surface temperatures at current values, while doubling the CO₂ at all levels. This experiment is thus similar to that of Boville (1986), except that here the full annual cycle is being used. As only the atmospheric concentration is changed, this run will be referred to as "ATM." Without allowing the sea surface temperatures to change, the doubled atmospheric CO₂ provides a greatly muted tropospheric warming of 0.37°C for the global, annual average.

There is currently substantial disagreement among the different modeling groups about the tropospheric latitudinal temperature response to doubled CO₂, a disagreement that could have a bearing on the middle atmosphere. The doubled CO₂ experiments run at the Geophysical Fluid Dynamics Laboratory (GFDL) (Manabe and Wetherald 1986) have produced a greater high latitude amplification (ratio of temperature change at high latitudes to that at low latitudes) than is the case in either the GISS or National Center for Atmospheric Research (NCAR) models. This difference affects the modeled changes in longwave energy in the troposphere, at least when the two different warming distributions are evaluated with the GISS model (Rind 1987). To cover the range of currently modeled tropospheric responses, we thus have a third experiment in which the atmospheric CO₂ concentration is doubled, and the sea surface temperatures are changed in such a way as to provide the model with the GFDL-type increased high latitude amplification. As discussed in Rind (1987), the procedure involves altering the latitudinal changes in sea surface temperature from the standard GISS doubled CO₂ run so as to provide the same global mean temperature warming as in this model (4.2°C) but with reduced warming at low latitudes, and increased warming with decreased sea ice at high latitudes. The longitudinal gradients in sea surface temperature from the standard doubled CO₂ run are retained. The intention is not to reproduce the GFDL doubled CO₂ tropospheric climate exactly, but simply to investigate the impact of high latitude amplification within the range currently being generated by different models. This altered doubled CO₂ run is referred to as "ALT."

These three experiments are each run for three years following a several-month-long spinup. As the sea surface temperatures are specified, the individual years for each experiment greatly resemble one another, and so can be averaged together. None of the models are in radiative equilibrium, however, which would require allowing the sea surface temperatures to adjust. The difference from equilibrium is most noticeable in ATM and ALT, since their patterns of sea surface temperature change are quite different from the GISS models' doubled CO₂ warming tendencies. Even 2CO₂ would have had a somewhat different response, however, if

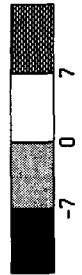
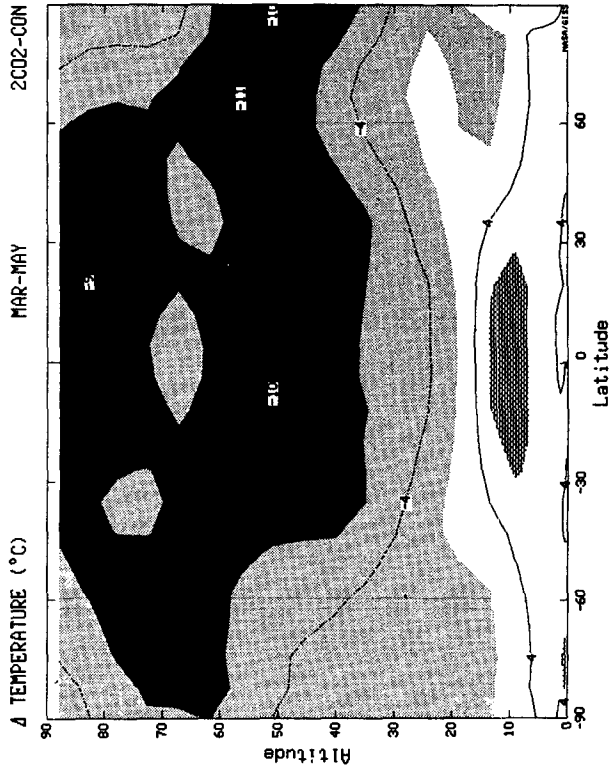
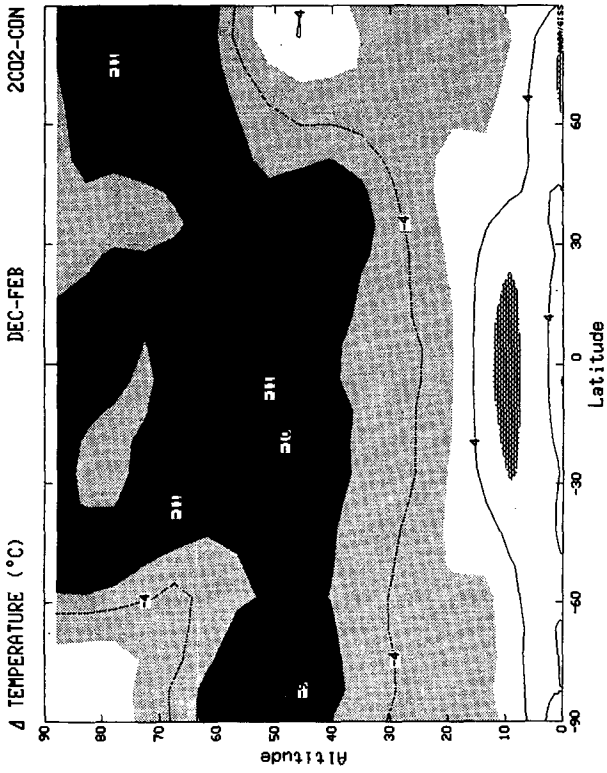
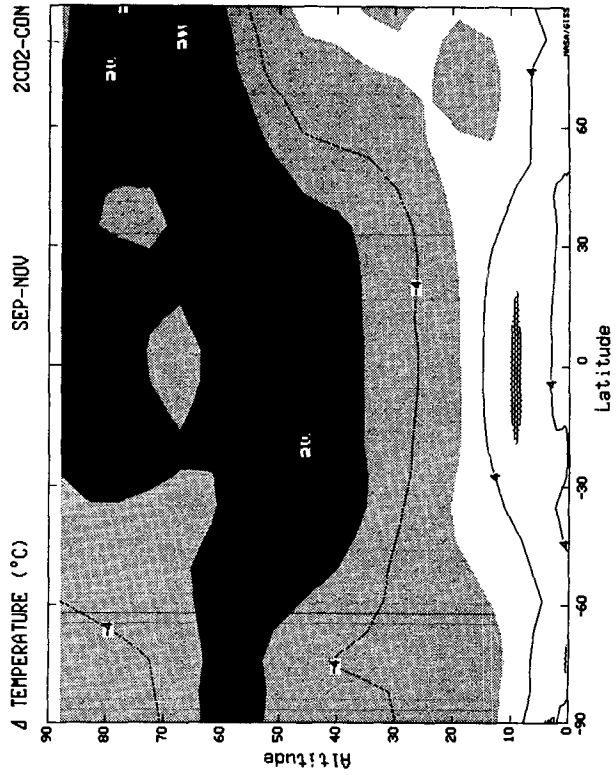
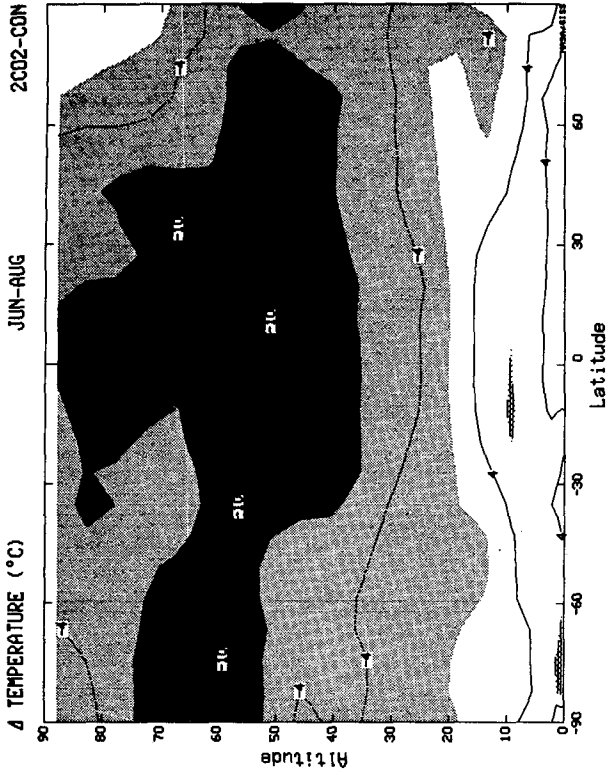
the sea surface temperatures were allowed to adjust. We will return to this point in section 4.

In order to ascertain if the middle atmospheric changes are primarily controlled by in situ effects or by changes in the troposphere, and to separate dynamical and radiative influences, several winters were rerun with CO₂ reset to 315 ppm above 100 mb. In the first rerun, referred to as "2CO₂-A," the sea surface temperatures were maintained at the values for the doubled CO₂ climate, and in the second rerun, referred to as "ATM-A," the sea surface temperatures were maintained at current values. An inverse experiment, in which CO₂ was doubled only in the stratosphere, was run for the last winter, and will be referred to as "STRAT." Finally, an experiment in which dynamics extended only up to 100 mb, limiting the middle atmosphere layers to their radiative response, was run for both single and doubled CO₂ atmospheric concentration with the respective boundary conditions. The doubled CO₂ run is referred to as "RAD."

A description of the different experiments is presented in Table 1. Conducting the range of experiments described above fulfills several objectives. First, the results (from ATM) can be compared with the few previous simulations that have been published. Furthermore, as the tropospheric doubled CO₂ simulations are showing a range of high latitude amplifications, the use of both 2CO₂ and ALT allow for tropospheric responses that highlight the current uncertainty in the distribution of the projected climate warming. Doubling the CO₂ only above or below 100 mb helps in separating the influence of the troposphere and stratosphere, and limiting the middle atmosphere to its radiative response allows us to distinguish between dynamic and radiative influences. Finally, many of the changes in stratospheric dynamics are found to be on

TABLE 1. Description of experiments.

2CO ₂	Doubled atmospheric carbon dioxide in troposphere and stratosphere, sea surface temperatures raised to values produced by doubled carbon dioxide equilibrium climate run.
ALT	Doubled atmospheric carbon dioxide in troposphere and stratosphere, sea surface temperatures raised to values more similar to GFDL doubled carbon dioxide climate run, with greater high latitude amplification.
ATM	Doubled atmospheric carbon dioxide in troposphere and stratosphere, sea surface temperatures specified at current values.
ATM-A	Like ATM, except doubled atmospheric carbon dioxide only in troposphere.
2CO ₂ -A	Like 2CO ₂ , except doubled atmospheric carbon dioxide only in troposphere.
STRAT	Like ATM, except doubled atmospheric carbon dioxide only in stratosphere.
RAD	Like 2CO ₂ except that above 100 mb, only radiation is calculated (no dynamics); also a control run for this experiment with 1 × CO ₂ .



the order of 10%–20% of the mean, with peak values of only several times the interannual standard deviations, and simulations would have to be run for many years to prove their significance. This is true of dynamic and hydrologic changes in the troposphere due to doubled CO₂ as well (Rind 1986, 1987, 1988a,b). The comparison of multiple experiments facilitates interpretation of the physical significance and mechanics of the changes.

Comparisons will be made between the experiments and the GCMAM control run (I, II). As noted in I, the first two years of the five year control run set the value of the coriolis parameter near the pole to zero, as was done in the standard UCLA model code from which the GISS numerical scheme was adopted (Arakawa 1972). The last three years used the full value of the coriolis parameter, as in GISS model II (Hansen et al. 1983). This difference affects the circulation near the pole. As the three doubled CO₂ experiments all used the full coriolis parameter, they will be compared with the last three years of the control run. When the results are compared with the full five years, the doubled CO₂ changes discussed in this paper, in general, remain unaltered. The standard deviations are taken from the full five years of the control run, in order to provide a more meaningful estimate at most latitudes. They do, however, overestimate the model's natural variability at the highest latitudes.

3. Results

In order to focus on the important aspects of the results, they are organized as responses to a series of questions. We concentrate on the main experiment (2CO₂), with the other experiments referred to when appropriate.

a. Question 1: Is it true that the middle atmosphere cools everywhere when carbon dioxide is doubled?

Greater CO₂ concentrations should lead to increased longwave radiation from the middle atmosphere, and cooler temperatures. The temperature changes produced in 2CO₂ for the different seasons are shown in Fig. 1. The basic character of the doubled CO₂ changes is very clear: strong warming in the troposphere, peaking in the GISS model in the tropical upper troposphere, and strong cooling through most of the middle atmosphere. The peak cooling values are on the order of 10°C in the tropical stratopause region. Cooling predominates in all seasons, and is thus in general agreement with expectations.

Warming occurs, however, in the Northern Hemisphere polar stratosphere during the colder half of the year. This is shown more clearly in Fig. 2, which gives the monthly average temperature changes at three levels: the lower stratosphere (68 mb), the upper stratosphere (1.5 mb), and the mesosphere (0.015 mb). The winter high latitude warming in the upper stratosphere is clearly evident in the Northern Hemisphere, and small warming occurs during Southern Hemisphere winter as well. Another small area of warming occurs in the mesosphere during summer in both hemispheres. (Above approximately 75 km the results may be severely affected by the breakdown of local thermodynamic equilibrium and the influence of the model top; an analysis of model limitations is provided in section 4.)

The polar warming is clearly not in agreement with expectations, and indicates that more is happening in the middle atmosphere in this experiment than simple radiatively induced temperature changes. To investigate what the radiative response would be by itself, an experiment was run in which for all levels above 100 mb only radiative transfer was allowed to influence the temperature, i.e., no dynamics was allowed to occur. This was done for both a control run, with 315 ppm CO₂ throughout and current sea surface temperatures, and an experiment (RAD), with doubled CO₂ throughout, and the warmer sea surface temperatures. The experiment was begun on 1 September, and integrated through the following winter; given that the thermal response time of the stratosphere is approximately 1 month, the spinup was sufficiently long to allow the full effects of the different radiative tendencies to be manifest.

The change in temperature for December–February between RAD and its control is shown in Fig. 3 (top). Now cooling occurs throughout the middle atmosphere, although again there is greater cooling in the equatorial stratosphere than in the polar night region. This latitudinal dependence is expected (Fels et al. 1980), since the radiative change will be larger where the control run temperatures were larger. The contrast between the December–February results shown in Figs. 1 and 3 indicate the role that changes in dynamics are playing in altering the temperature profiles.

We can look at this more directly by calculating how the temperature is changed by the model “dynamics” subroutine, in comparison with what occurs in the current climate control run. This result is shown in Fig. 3 (middle). The winter polar warming is a result of changed dynamical heating (as is the mesospheric

FIG. 1. Latitude–altitude depiction of the seasonal temperature change for the doubled CO₂ climate experiment (2CO₂) compared with the current climate control run: December–February (top left), March–May (bottom left), June–August (top right); September–November (bottom right). The format shown is used for most of the following figures: negative values are shaded, with more extreme negative values in the dark shading; more extreme positive values are shown by the brick pattern. The transition values are given by the bar legend at the bottom of the figure. Selected contours are shown (with the negative values dashed), as well as extreme negative and positive magnitudes. The changes are for 3-year averages for each of the experiments and the control.

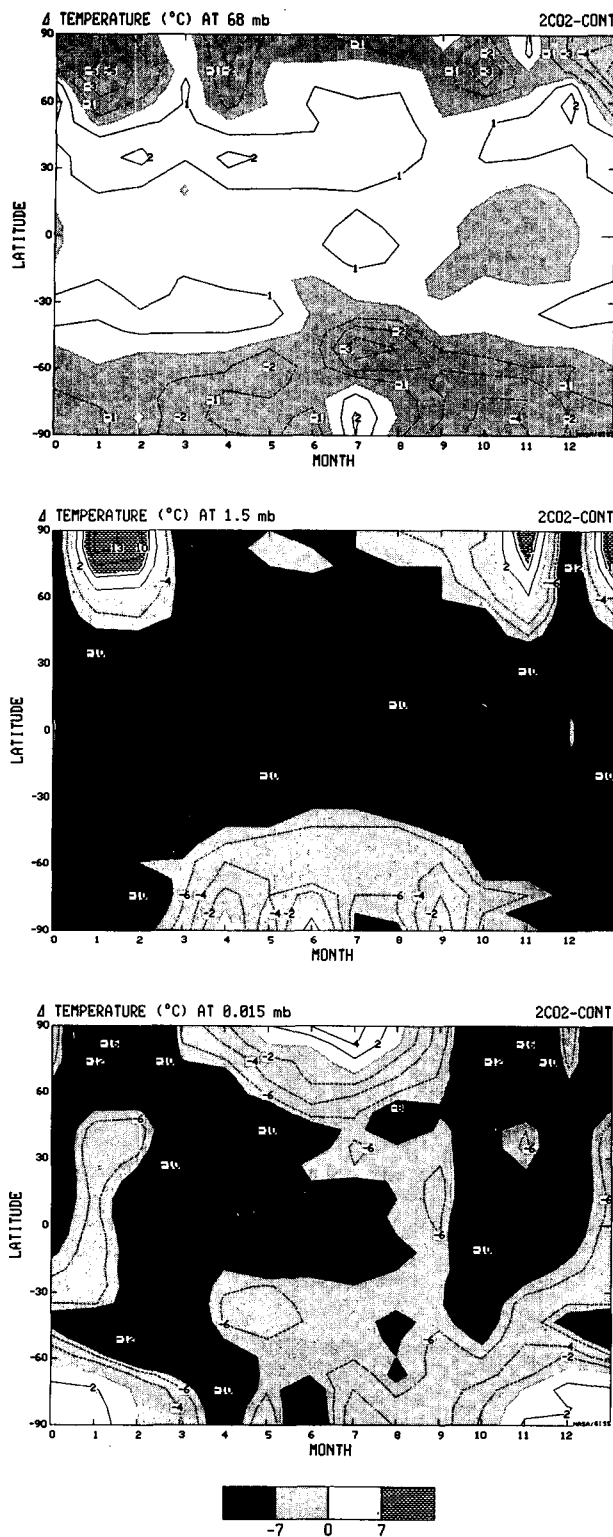


FIG. 2. Change of temperature as a function of month in 2CO₂ at 68 mb (top), 1.5 mb (middle), and 0.015 mb (bottom).

warming near the summer pole). More specifically, it is a result of a change in heating induced by the transformed Eulerian (residual) circulation [defined, for

example, in I, Eq. (23)] (Fig. 3, bottom). This implies that the residual circulation has changed in the doubled CO₂ climate.

Finally, we can ask how sensitive the results are to the exact specification of changes in the troposphere. Presented in Fig. 4 are the temperature changes which resulted during December–February in ATM (top), where the atmospheric CO₂ was doubled but sea surface temperatures left unchanged. Again warming appears near the winter polar stratopause. If CO₂ is doubled only in the troposphere, with or without the increased sea surface temperatures (2CO₂-A; ATM-A), the same pattern results. Doubled CO₂ in the stratosphere alone [STRAT, Fig. 4 (middle)] likewise results in polar warming. Only in ALT, with doubled CO₂ and the greater high latitude amplification of the sea surface temperature changes does actual warming not appear at the poles, just reduced cooling (Fig. 4, bottom). The dynamical warming thus seems to result from the vertical differentiation of the radiative effects of increased CO₂.

b. Question 2: What happens to the residual circulation in the middle atmosphere in the doubled CO₂ climate?

The change in residual circulation is shown in Fig. 5 for the different seasons, with negative (shaded) values indicating greater clockwise flow. In all seasons, in both hemispheres, the middle atmosphere residual circulation increases (i.e., greater equator to pole flow at high levels, with return flow at low levels), with changes on the order of 10% of control run values (2–3 standard deviations). This pattern, with greater poleward heat advection near the stratopause, and greater subsidence near the poles, is responsible for the dynamical polar warming shown in Fig. 3 (bottom). Why does this happen?

The residual circulation is driven by diabatic, eddy and gravity wave effects. The increased residual circulation could result from stronger diabatic heating at low latitudes compared with higher latitudes, or, given that it is the longwave radiative component which is directly affected with increased CO₂, decreased longwave cooling at low latitudes compared with higher latitudes. As implied by the temperature changes in Fig. 4 (top), this is not what is happening radiatively, at least in the winter hemisphere, for the low latitudes experience greater increase in radiative cooling.

Increased poleward flow near the stratopause could result from greater eddy forcing (stronger EP flux convergences), or stronger gravity wave drag. Both factors are occurring. Shown in Table 2 are the changes in the transformed streamfunction values for the experiments listed in Table 1, and the relative contribution to the change generated by the eddy and gravity wave effects. They were derived in the following manner: for each experiment the location of the maximum residual circulation change in the stratosphere was determined,

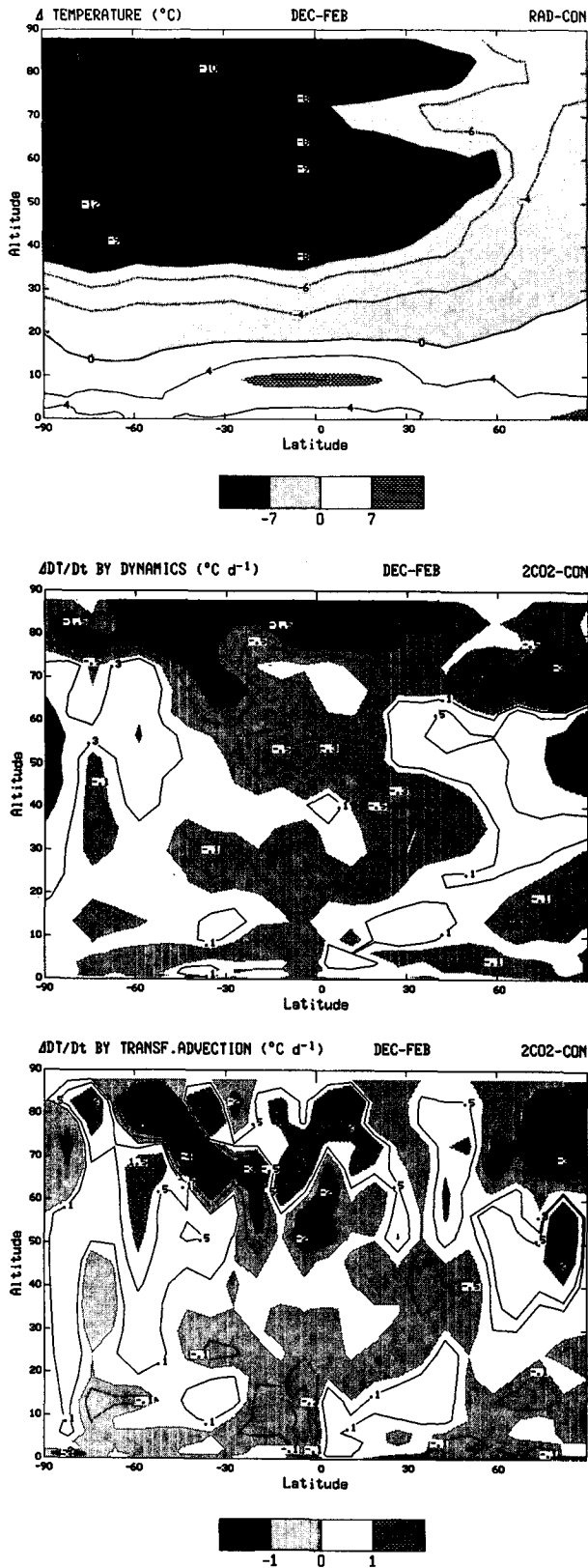


FIG. 3. Change of temperature in December–February between RAD and its control run (top). Difference of temperature changes

and also the location of the maximum change poleward of 50°N. The streamfunction maximum indicates that poleward mass flow was greatest in the atmosphere above that altitude. As EP flux convergence and the gravity wave drag help generate poleward mass flow [I, Eq. (22)], we integrate the magnitudes of those terms at all levels above the streamfunction maximum, and convert the values to a mass flow equivalent. Were these two forcing functions to generate the total mass flow, the sum of their values would equal the streamfunction value shown in Table 2, as is approximately true for the control run. Deviations can arise because the EP flux diagnostic must be averaged to the latitude of the streamfunction maximum, and other terms in the equation are not necessarily zero.

All the experiments show increased residual circulation intensity, often of two standard deviations or more (the value in parentheses), including the experiments in which CO₂ is doubled only in the troposphere (ATM-A, 2CO₂-A) or stratosphere (STRAT). The forcing appears to be due primarily to eddy effects at the higher latitudes, but to a combination of eddy and gravity wave effects at midlatitudes. Table 2 indicates that the increased gravity wave drag in the middle atmosphere is playing a substantial role in accelerating the residual circulation. In the control run it represents about one-third of the dynamical forcing in midlatitudes, and at high latitudes about one-fifth. In 2CO₂ it is the dominant term at the location of the midlatitude maximum circulation change. At polar latitudes, EP flux convergences in the upper stratosphere, and divergences in the lower stratosphere, act effectively to intensify poleward flow aloft and equatorward flow below, and eddies represent the chief forcing for circulation changes. This is not true in ALT with its altered energy propagation and EP flux divergences (discussed below).

c. Question 3: Why is the eddy forcing increasing?

Shown in Fig. 6 is the change in eddy energy during December–February in 2CO₂, ATM and ALT, along with the standard deviation of this quantity in the control run. Eddy energy increases through most of the middle atmosphere in all three experiments. The change for each hemisphere in each season is quantified in Table 3, with the results divided into four vertical regions. For the 24 cases shown in each region (three experiments, four seasons, two hemispheres), in 21 of the cases tropospheric energy decreased. Nevertheless, in 19 of these cases, eddy energy increased in the middle atmosphere, with the same percentage of increase in each of the three middle atmosphere regions.

Also included in Table 3 (as the numbers shown in

for December–February, 2CO₂ minus control, by the model dynamics (middle) and by the transformed advection (bottom).

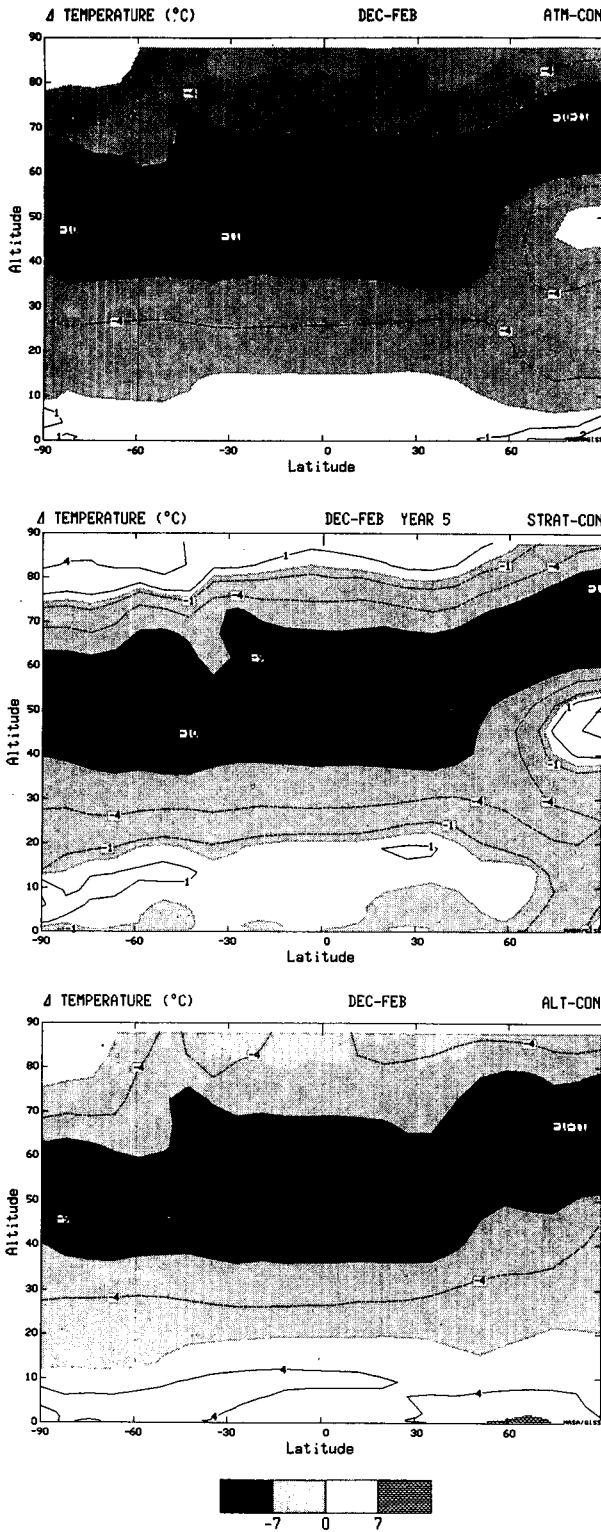


FIG. 4. Temperature change for December-February in ATM (top), STRAT (middle), and ALT (bottom).

parentheses), are the percentage changes in standing plus transient eddy kinetic energy for waves 1-3. In two-thirds of the cases, planetary longwave energy de-

creases in the troposphere (and a similar result arises if only standing longwave energy is included). Nevertheless, again for about 80% of the cases, the longwave energy increases in the middle atmosphere, and, in the lower stratosphere, it increases in 23 of the 24 situations. The conclusion that eddy energy is really increasing in the middle atmosphere is significant at greater than the 95% level when tested with a binomial distribution analysis of increase versus decrease.

How does this increased eddy energy arise? The winter energy budgets for the Northern Hemisphere troposphere and lower stratosphere are given in Table 4. Note that in all three experiments standing wave 1 eddy energy increases in the troposphere, despite the overall reduction in tropospheric eddy kinetic energy which occurs when sea surface temperatures are increased, the latitudinal temperature gradient decreases, and baroclinicity is reduced (Table 4, EAPE → EKE). The warming of the lower troposphere and cooling of the lower stratosphere (Figs. 1, 4) decreases the vertical stability. This leads to an overall increase in available potential energy for the longest waves, which are capable of being more strongly influenced by the large-scale vertical static stability changes than are the smaller scale eddies. For example, at 45°N, tropospheric eddy available potential energy for wavenumber 1 increases an average of 10% in the three experiments during winter. For the Northern Hemisphere as a whole, baroclinic generation of wavenumbers 1-2 increase by 16% in ALT, and in 2CO₂, baroclinic generation of wavenumbers 1-6 increase by 8%. The standing wave 1 energy increase is large relative to the mean value (25%-50%) and greater than or equal to two times the standard deviation.

In all three experiments the increased wave 1 energy is also found at higher levels, although in ALT the specification of warm high latitude oceans provides for increased wavenumber 2 stationary eddy energy as well. To illustrate the paths followed by the eddies with increased energy, changes in the EP flux for the different experiments are presented in Fig. 7, along with the change in the zonal wind. In the troposphere, increased vertical propagation starts mainly at the upper mid-latitudes where eddy energy increases (Fig. 6). Its path into the middle atmosphere is determined by changes in the refraction characteristics associated with the changed wind structure, basically propagating through regions of relative west wind increase. The differences among the experiments in the tropospheric zonal wind response are associated via the thermal wind relation to the differences in heating produced with the warmer sea surface temperatures (e.g., the large high latitude heating prescribed in ALT leads to reduced west winds at upper midlatitudes). The increased stratospheric west winds, where they occur, are associated with the stronger transformed advection (Fig. 5) and greater EP flux divergences (Fig. 8), while the decreased mesospheric west winds are due to greater EP flux convergences and increased gravity wave drag.

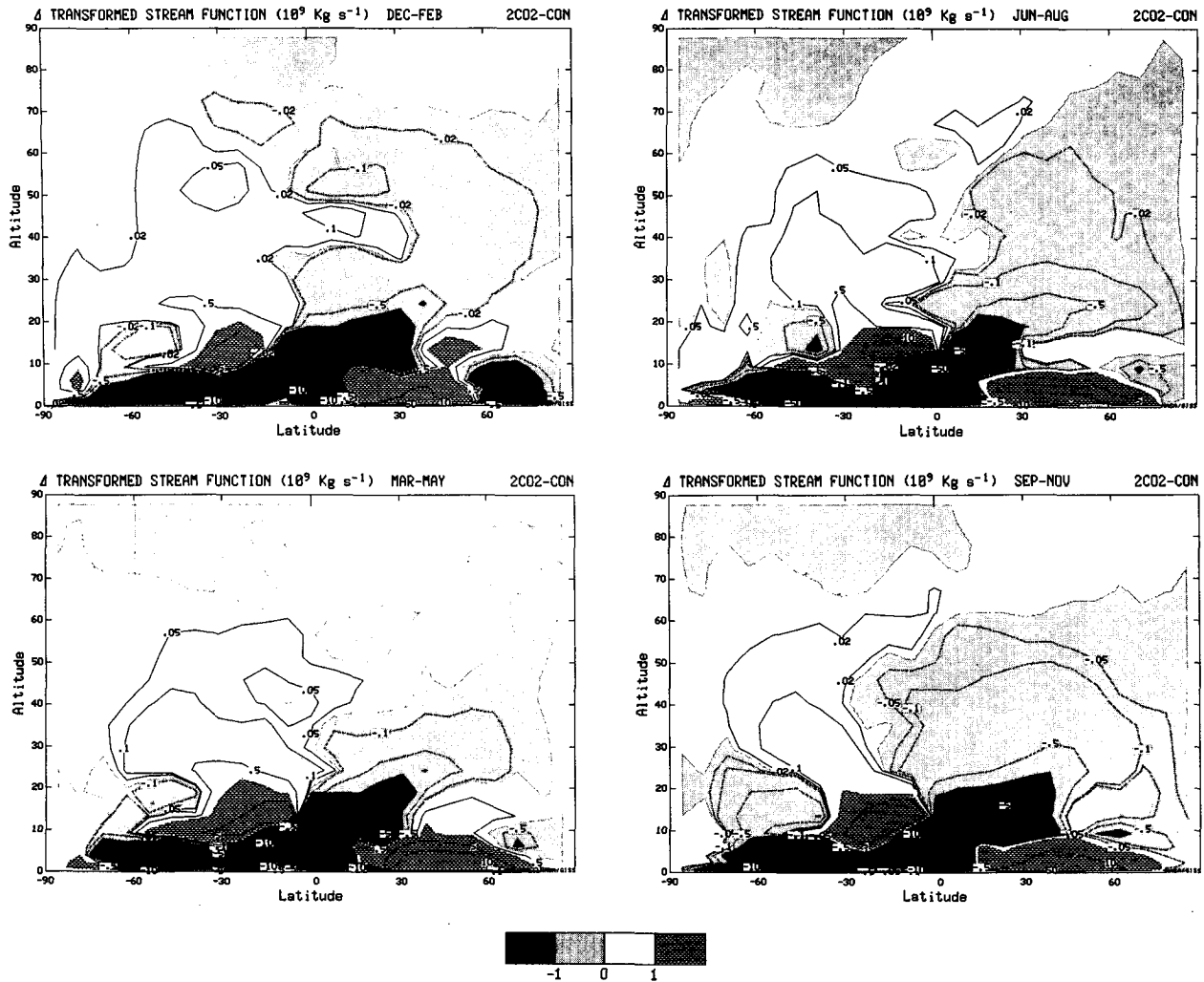


FIG. 5. Change in the transformed (residual) circulation in 2CO₂ for December–February (top left), March–May (bottom left), June–August (top right) and September–November (bottom right). A negative (positive) change in the Northern (Southern) Hemisphere indicates an increased direct circulation from equator to pole.

The patterns of energy flow are also influenced by tropospheric eddy energy changes, with ATM and ALT having the greatest high latitude tropospheric increase. Thus in 2CO₂ the energy flow change in the middle atmosphere is towards high latitudes, while in ALT the change in propagating energy is upward at and then away from the highest latitudes. Nevertheless, there is an overall pattern for increased upward fluxes at high latitudes in all the experiments, with peak vertical flux changes 10%–20% of control run values (three standard deviations).

The amount of eddy energy increase that is occurring through increased direct generation versus increased propagation varies with season (e.g., vertical propagation is not a contributing factor during the summer season when east winds limit upward penetration). Analysis of the different experiments indicates the following generalities. Lower stratospheric planetary longwave energy increases appear to be associated with

increased generation as well as increased propagation from the troposphere when that is available. The increased generation results from increases in potential energy, a direct result of the general decrease in vertical stability, with tropospheric warming and stratospheric cooling, as well as the greater high latitude cooling in the region from 200 to 50 mb (Fig. 1). For example, in the lower stratosphere at 45°N, the annual average wavenumber one available potential energy increases by an average of about 10% in the three experiments. The increased energy in the lower stratosphere then propagates vertically.

These results help explain the increased eddy forcing of the residual circulation. Shown in Fig. 8 are the changes in EP flux divergences in 2CO₂ for the different seasons. The increased eddy energy in the lower stratosphere leads to increased EP flux convergences at higher levels; the increased eddy forcing then helps generate a more direct streamfunction in the middle atmosphere

TABLE 2. Middle atmosphere residual circulation and changes, December–February. Note: Change results are for the last winter.

Maximum streamfunction and change (10^7 Kg s^{-1})				
Run	Location	Trans. S.F.	Eddy	Gr. wave
Control	(39°N, 46 mb)	-419 (± 24)	-294	-124
$\Delta 2\text{CO}_2$	(39°N, 46 mb)	-93	-41	-90
$\Delta 2\text{CO}_2\text{-A}$	(39°N, 46 mb)	-168	-87	-120
ΔATM	(39°N, 46 mb)	-101	-108	-29
$\Delta \text{ATM-A}$	(31°N, 46 mb)	-42	-23	-57
ΔSTRAT	(16°N, 21 mb)	-41	-35	11
ΔALT	(39°N, 46 mb)	-62	-45	-30

High latitude maximum streamfunction and change (10^7 Kg s^{-1})				
Run	Location	Trans. S.F.	Eddy	Gr. wave
Control	(55°N, 46 mb)	-278 (± 12)	-236	-66
$\Delta 2\text{CO}_2$	(55°N, 10 mb)	-30	-47	-7
$\Delta 2\text{CO}_2\text{-A}$	(55°N, 46 mb)	-40	-66	23
ΔATM	(70°N, 46 mb)	-32	-50	-6
$\Delta \text{ATM-A}$	(70°N, 21 mb)	-7	-3	-5
ΔSTRAT	(55°N, 10 mb)	-18	-16	-4
ΔALT	(55°N, 46 mb)	-21	8	-11

of both hemispheres, which leads to warming of the polar latitudes (Fig. 3). The mesosphere responds to the increased poleward flow near the stratopause with a more indirect circulation, increased rising air and cooling in the winter polar mesosphere, increased sinking air and warming in the summer polar mesosphere. The differences in magnitude of high latitude warming among the different experiments are associated with the different patterns of EP flux convergence (Fig. 7) and thus residual circulation change.

d. Question 4: How do changes in gravity wave drag affect the results?

As indicated in Table 2, increased gravity wave drag is partly responsible for increases in the midlatitude residual streamfunction. The gravity wave changes, as parameterized in the model (I), will result from changes in the source and in propagation and breaking characteristics. In 2CO_2 the parameterized source strengths for gravity waves, mountain waves, wind shear, and convection, all increase. In this experiment there is a general increase in west winds in the troposphere (note the increase in zonal kinetic energy in Table 4), which leads to greater mountain wave and shear wave generation. Also, as climate warms, penetrating convection increases, which increases the amplitude of the high phase velocity gravity waves. As indicated by the zonal wind changes shown in Fig. 7, however, the zonal winds in the lower stratosphere also increase in intensity (due, via the thermal wind relationship, to the large upper troposphere tropical warming), which makes breaking more difficult. The stronger waves break higher up, and increase the gravity wave drag by 10%–50% of control run values, an effect

which becomes as large or larger than any other individual influence in the upper mesosphere. In ALT, zonal kinetic energy decreases (Table 4) due to its greater high latitude amplification of the temperature change, as do mountain and shear wave sources, so the gravity wave changes are somewhat less important (Table 2).

e. Question 5: Do stratospheric sudden warmings change in the doubled CO_2 climate?

With the change in eddy energy, and the alterations in propagation characteristics, the possibility arises that dynamic events in the stratosphere may be altered. This in fact does happen, and is part of an overall pattern of change that occurs in both hemispheres. The *sudden warming* events are defined here as events involving large and rapid increase of eddy kinetic energy and decrease of zonal kinetic energy (examples of such events in the control run were given in II). In the control run, sudden warmings occurred in December, while in the doubled CO_2 experiments, sudden warmings occurred one month earlier, then repeat again in January/February, leading to a delay in the final spring warming. These changes occur in 2CO_2 , ATM and ALT.

To explain how these changes arises, we discuss the wintertime evolution of events forced by the climate change, concentrating first on the Northern Hemisphere. The main points of the following discussion are shown schematically in Fig. 9, which indicates the regions of high latitude warming and cooling as a function of month, as well as the altitudes of increased upward propagation of planetary waves, as determined from the change in the vertical EP flux. The actual deceleration of the zonal wind with warming at high latitudes is associated with the convergence of the EP flux, and thus better approximated by the warming regions themselves. The warming referred to in Fig. 9 is calculated relative to the control run, and is often, though not always, associated with the actual sudden warming events. We discuss the monthly changes sequentially.

1) NOVEMBER

During this month the sun is sufficiently close to the equator, and sea surface temperatures sufficiently warm in the tropical Northern Hemisphere, that increased penetrating convection in the doubled CO_2 experiments causes substantial heating of the tropical and subtropical Northern Hemisphere upper troposphere. This warming increases the subtropical latitudinal temperature gradient, and thus, from the thermal wind relation, increases the zonal winds in the upper troposphere and lower stratosphere at subtropical and lower middle latitudes. In contrast, winds at these levels do not increase as much (or actually decrease) at higher latitudes, as the albedo-driven high latitude amplifi-

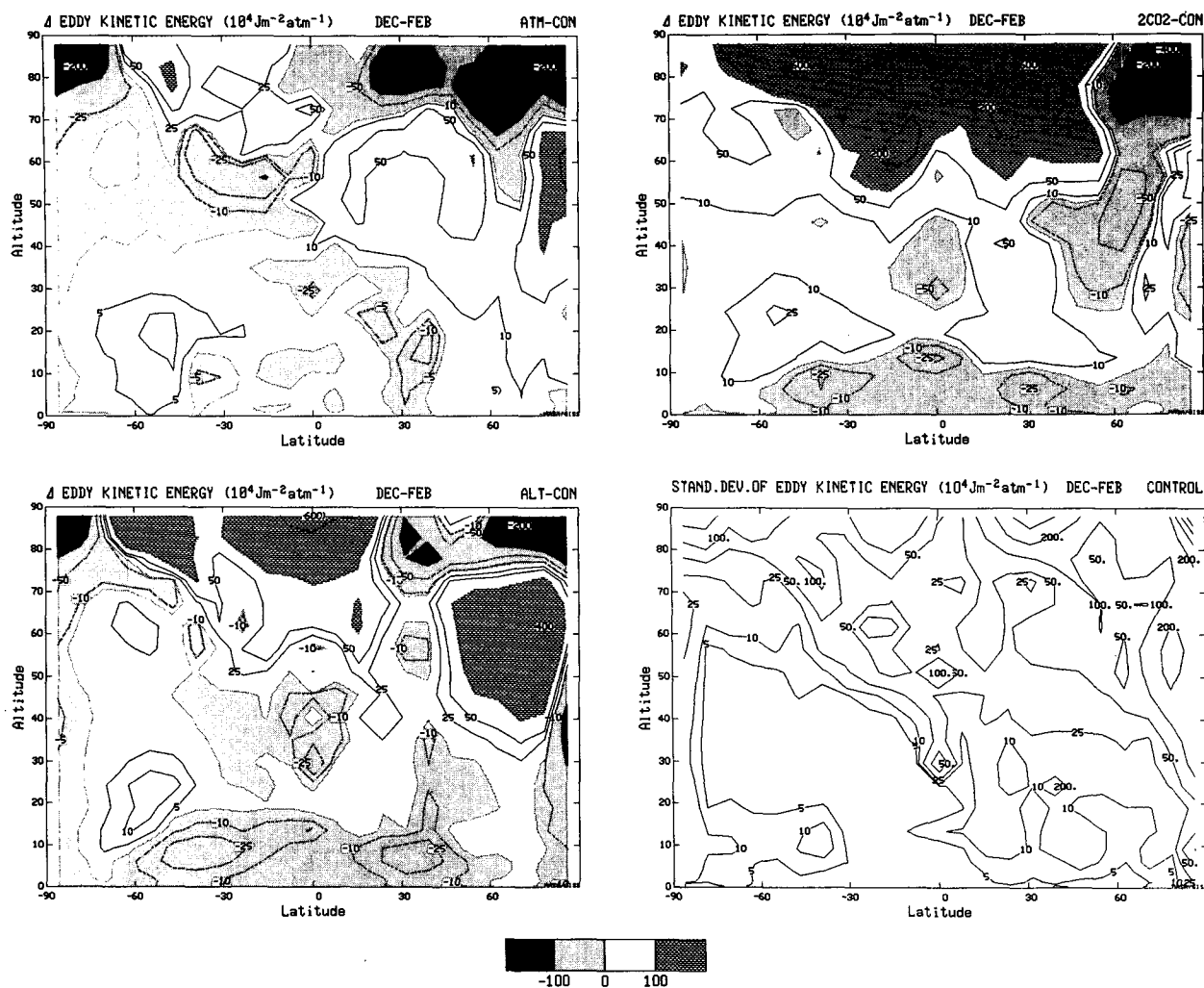


FIG. 6. Change in the eddy kinetic energy for December–February in ATM (top left), ALT (bottom left), 2CO₂ (top right) along with the interannual standard deviation from the control run (bottom right).

cation of the temperature response reduces the extratropical latitudinal temperature gradient. The change in wind response with latitude sharpens the subtropical jet stream, altering the refractive properties of the atmosphere so as to allow wave energy to propagate from the upper troposphere into the middle atmosphere more easily.

The additional eddy energy in the stratosphere intensifies the residual circulation and warms the higher latitudes associated with sudden stratospheric warming events. The same events also produce cooling in the mesosphere, a response noted in simulations of sudden stratospheric warmings in the control run (II), and one which has often been observed (e.g., van Loon et al. 1975).

2) DECEMBER

The reduction in the hemispheric latitudinal temperature gradient that accompanies the tropospheric

warming leads to reduced eddy energy, and reduced eddy deceleration of the upper tropospheric zonal winds at higher latitudes. As these winds increase, and as the tropical heating moves southward, the refraction properties now change so as to make upward propagation less favorable. Less eddy energy propagates out of the troposphere, stratospheric eddy energy decreases, and polar temperatures cool. At upper levels, above approximately 0.10 mb, the mesospheric polar region recovery from the cooling events of the preceding month decreases high latitude west winds, which allows for increased upward energy propagation. This increased eddy energy leads to increased transformed advection, which warms polar levels at mesospheric heights.

The eddy energy decrease responsible for the tropospheric wind changes occur in November from decreased baroclinicity; during December, longwave energy starts increasing, due to the effect of decreased tropospheric stability as discussed above. Tropospheric

TABLE 3. Percentage change in eddy energy (waves 1-3 in parentheses).

	Troposphere	Lower strat	Upper strat	Mesosphere
Northern Hemisphere				
Winter				
ATM	1.9 (3.9)	2.4 (5.3)	7.5 (10.4)	3.5 (2.6)
2CO2	-4.7 (6.4)	10.2 (22.9)	1.9 (-0.2)	9.8 (7.9)
ALT	-9.3 (-1.7)	-0.0 (0.5)	6.7 (7.7)	8.6 (11.3)
St. dev.	3.7	2.8	5.4	5.6
Spring				
ATM	-1.6 (-2.3)	-1.1 (-2.3)	-13.4 (-19.7)	-8.3 (-12.2)
2CO2	-6.0 (2.4)	15.0 (30.4)	-7.2 (-12.4)	6.2 (10.6)
ALT	-14.7 (-9.1)	5.3 (9.1)	-4.4 (-10.5)	-1.4 (-4.7)
St. dev.	1.9	3.1	7.5	4.2
Summer				
ATM	-2.9 (4.2)	7.1 (16.7)	0.2 (1.2)	-0.3 (-1.8)
2CO2	-13.2 (-12.7)	37.6 (58.5)	4.4 (-1.1)	9.4 (11.3)
ALT	-14.2 (-3.9)	20.1 (29.7)	5.6 (3.9)	3.3 (0.8)
St. dev.	1.5	3.0	7.3	1.9
Fall				
ATM	-2.8 (-0.9)	0.6 (0.3)	0.2 (2.6)	3.4 (4.9)
2CO2	-11.2 (-1.7)	13.3 (32.5)	17.3 (21.6)	19.5 (24.5)
ALT	-12.8 (0.3)	4.0 (17.6)	9.5 (14.4)	17.9 (23.1)
St. dev.	2.2	6.2	4.0	5.8
Southern Hemisphere				
Winter				
ATM	-0.7 (-1.8)	6.9 (9.0)	16.1 (14.8)	7.7 (11.3)
2CO2	-10.4 (-9.3)	-0.4 (1.3)	1.9 (1.2)	2.4 (0.3)
ALT	-15.3 (-13.0)	-1.3 (7.0)	3.1 (6.8)	-4.6 (-7.2)
St. dev.	4.0	4.3	10.1	1.6
Spring				
ATM	-2.2 (-0.9)	5.1 (10.0)	10.0 (14.7)	3.9 (4.8)
2CO2	-12.4 (-3.7)	2.6 (15.1)	6.7 (11.0)	16.9 (19.0)
ALT	-18.5 (-18.3)	-3.6 (1.6)	12.2 (20.9)	8.6 (8.7)
St. dev.	1.4	5.3	7.9	3.1
Summer				
ATM	2.0 (3.6)	12.6 (17.9)	-1.2 (-4.7)	-3.0 (-4.2)
2CO2	-7.0 (0.2)	28.3 (40.7)	8.4 (11.0)	19.1 (24.7)
ALT	-17.4 (-13.7)	7.0 (16.8)	-2.2 (-2.0)	5.9 (7.6)
St. dev.	4.4	5.9	5.8	0.8
Fall				
ATM	0.2 (-2.3)	3.9 (9.8)	4.7 (9.2)	2.2 (5.0)
2CO2	-11.6 (2.2)	12.9 (33.3)	3.6 (8.4)	16.8 (23.6)
ALT	-15.5 (-9.9)	0.4 (7.7)	3.4 (7.8)	6.6 (10.2)
St. dev.	3.8	4.6	6.3	1.2

stability decreases more in winter than fall because the tropospheric stability is currently greater in winter, and therefore can trap more heat near the surface. In addition, winter sea ice is greater, so there is more sea ice to lose as climate warms, and more heating from absorbed solar radiation and ocean ventilation which can occur because of its loss.

3) JANUARY

Some tropospheric longwave planetary energy increase occurs in this month, but, on the other hand, the winter subtropical heating is less, and the latitudinal

temperature gradient suffers its maximum decrease. This results in a reduction of the latitudinal gradient of potential vorticity, and more unfavorable propagation conditions. The effects work against one another, with the result that eddy energy propagates more easily only from the upper troposphere. Nevertheless, this additional energy for the stratosphere increases the residual circulation, and is associated with sudden warming events. Again the response of the mesosphere is to cool.

4) FEBRUARY

Tropospheric longwave energy increases occur in this month, but now it is not primarily the result of decreased stability. By this time of the year, the solar radiation is returning to the tropical Northern Hemisphere, and the increased tropical warmth of the doubled CO₂ climate intensifies the Hadley Circulation. The energy transfers that accompany this process, and the increased temperature gradient associated with tropical heating, provide for greater energy transfers from zonal available potential energy to zonal kinetic energy, and then from zonal kinetic to eddy kinetic energy. Decreased stability helps this latter process, as it allows the gradient of quasi-geostrophic potential vorticity to become negative occasionally, promoting barotropic instability. In the stratosphere, polar warming occurs during this month, weakening the west winds, which further enhances energy propagation. Cooling again characterizes the mesosphere, with reduced propagation characteristics.

Note that here a distinction arises among the experiments, for due to its relatively cool equatorial sea surface temperatures, ALT does not show an increase in the Hadley circulation, zonal kinetic energy, or longwave energy. Thus in this run increased vertical propagation of eddy energy arises only above the mid-troposphere, while in the other two experiments it occurs from the surface.

5) MARCH

The eddy energy increase in February is sufficiently strong that it decelerates the midlatitude tropospheric west winds, an effect which becomes apparent by March, and results in less favorable vertical propagation conditions. This, combined with smaller increases in tropospheric longwave energy, leads to reduced eddy energy propagation into the middle atmosphere and cooler conditions in the stratosphere. As was the case in December, the mesospheric response is to warm, with better propagation conditions allowing more eddy energy. The relative cooling of the stratosphere in March indicates a delay in the onset of the final warming as compared to the control run, which is consistent with the later midwinter warmings in the modeled doubled CO₂ climate.

The overall pattern shown in Fig. 9 depicts an apparent downward propagation of regions of relative

TABLE 4. Northern Hemisphere December–February energy budgets, troposphere and lower stratosphere. KE: Kinetic energy; APE: Available potential energy; E: Eddy; Z: Zonal; G: Generation; D: Destruction; energy (10^{17} J); rates (10^{12} W).

	Control	Δ ATM	Δ 2CO ₂	Δ ALT	Std. dev.
Troposphere (984–100 mb)					
EKE	2809	52.3	-132.5	-260.1	105.0
Stationary EKE	838	50.0	-11.5	-17.2	32.3
Standing wave 1 EKE	140	65.6	54.5	36.9	19.6
ZKE	1728	68.2	325.9	-122.9	22.7
EAPE	6957	32.3	-518.3	-145.5	116.0
ZAPE	12920	-173.3	-157.0	-1911.4	259.3
EAPE → EKE	681	9.0	-68.0	-89.0	37.8
ZAPE → ZKE	162	9.0	19.9	-1.5	31.1
ZKE → EKE	-39	10.0	15.1	15.9	19.5
GEAPE	581	-57.8	-163.0	-53.0	27.1
GZAPE	1507	-88.6	-256.1	-355.8	45.2
DEKE	411	-10.8	13.3	22.4	10.0
DZKE	192	-5.2	-11.1	6.5	5.9
Lower stratosphere (100–10 mb)					
EKE	288	6.8	29.3	-0.1	8.2
Stationary EKE	78	0.3	5.8	10.1	2.4
Standing wave 1 EKE	17	5.1	9	3.3	6.1
ZKE	218	67.9	150.5	-9.2	34.4
EAPE	328	12.8	13.1	-0.5	6.4
ZAPE	201	-22.3	-10.4	-16.9	18.2
EAPE → EKE	-72	2.8	0.1	4.5	6.2
ZAPE → ZKE	15	1.5	13.3	4.4	0.9
ZKE → EKE	3	-2.3	1.5	1.9	1.3
GEAPE	-16	-2.5	-0.6	-0.3	1.8
GZAPE	-12	5.1	-2.4	-0.7	2.7
DEKE	9	-0.4	-2.1	0.1	1.2
DZKE	18	4.4	14.0	2.5	1.7
$\omega'\phi'$ at 100 mb	112.5	-2.2	-0.28	-11.7	6.9

warming and cooling, starting in September and continuing through April. A similar phenomenon occurs in the polar Southern Hemisphere, with relative warming propagating down in time from the mesosphere in May to the lower stratosphere in July (see Fig. 2). The explanation follows a similar pattern; for example, upward energy propagation from the troposphere to the midstratosphere occurs in June, when increased longwave propagation coincides with more favorable propagation conditions.

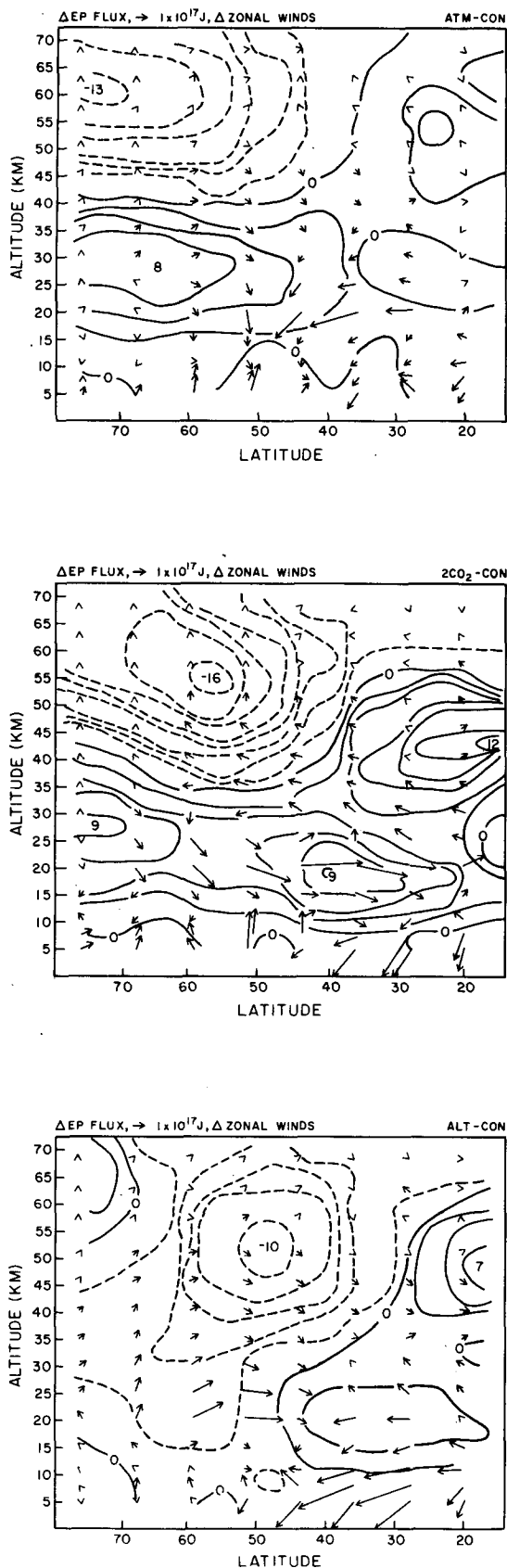
Notice that the Southern Hemisphere winter changes are one month later in phase than those for Northern Hemisphere winter (e.g., warming in the midstratosphere in June in the Southern Hemisphere, in November in the Northern Hemisphere). This delay appears to be related to the hemispheric differences in the control run latitudinal precipitation patterns. In the Northern Hemisphere, for the current climate, the model produces maximum rainfall at 20°N in November; in the equivalent Southern Hemisphere month (May) maximum rain occurs near the equator. The difference is associated with the greater land/ocean ratio in the Northern Hemisphere, which draws the intertropical convergence zone further poleward during summer.

In the doubled CO₂ climate, the increased heating

due to moist convection amplifies processes evident in the control run, and thus the *change* in heating also occurs further poleward in the Northern Hemisphere in November than in the Southern Hemisphere in May, as does the maximum upper troposphere zonal wind increase and refraction changes. Hence the increased vertical energy propagation in November in the Northern Hemisphere at middle latitudes does not occur in the Southern Hemisphere in May. The Southern Hemisphere middle atmosphere actually experiences reduced eddy energy in May, reduced eddy deceleration of the winds (both opposite to the Northern Hemisphere changes in November), and thus increased west winds at higher latitudes by June. This wind change provides favorable conditions for vertical and poleward energy propagation during June, with increased middle atmosphere eddy energy and relative warming.

f. Question 6: Is the change in the timing of stratospheric warmings due primarily to alterations in tropospheric processes or to the stratospheric cooling?

A change in the average timing or characteristics of stratospheric warmings would have important consequences for ozone transport (e.g., Leovy et al. 1985). If this is a real change, alterations in the eddy energy



propagation patterns as discussed above are one explanation. Another possibility exists: perhaps the change in timing of the warming events was influenced by radiation effects. There are at least two potential causes. The additional radiative dissipation of planetary waves which arises when CO_2 is increased in the stratosphere may help warmings to reach fruition both earlier (November) and then again later than in the control run. The impact of increased dissipation (from gravity waves) in promoting stratospheric warmings in the control run has been discussed previously (II). Alternatively, Fels (1985) has noted that the N30 version (3° horizontal resolution) of the GFDL SKIHI GCM underwent warming episodes on the same date in two successive model years, which he suggested might be associated with overly strong radiative control of the polar temperature; the preconditioning of the polar vortex, which is normally associated with minor warming events, might be arising in the model mostly from the seasonal cooling, thus producing a phase lock of the preconditioning and warming with the annual cycle. It is possible that the increased CO_2 might precondition the model atmosphere to experience warmings at an earlier time.

The descriptions for the winter patterns given above emphasize processes strongly influenced by tropospheric events, with low latitude heating changing the atmospheric refractive properties, and altered tropospheric stability and latitudinal temperature gradients affecting longwave generation and propagation. In fact, the increased CO_2 in the stratosphere does not appear in the discussion, except for its influence on tropospheric stability. If this is true, then somewhat similar results should arise whenever these tropospheric changes occur, regardless of what is happening radiatively in the stratosphere.

To test this assumption, we can investigate the timing of the stratospheric warmings in the experiments in which CO_2 was increased only in the troposphere (ATM-A; 2CO2-A). In the three winters for which these experiments were run, the sudden warming events occurred close to the control run times, in December. It might thus appear that this result verifies the importance of increased radiative cooling, except that in STRAT, with CO_2 doubled only in the stratosphere, the warming again occurred only in December. Thus, the change in timing of the warmings noted in 2CO2, ATM and ALT arose only in those runs in which CO_2 was doubled in both regions.

FIG. 7. Change of the EP flux (arrows) and the zonal wind changes (contours) for December-February in the Northern Hemisphere. The length scale for the arrows is shown in the top left-hand corner of each figure; values below 20 km are reduced by a factor of 10 for presentation purposes. Negative zonal wind changes are dashed, and selected peak magnitudes of wind change are shown. Note that in contrast to the other figures, the Northern Hemisphere latitudes increase to the left.

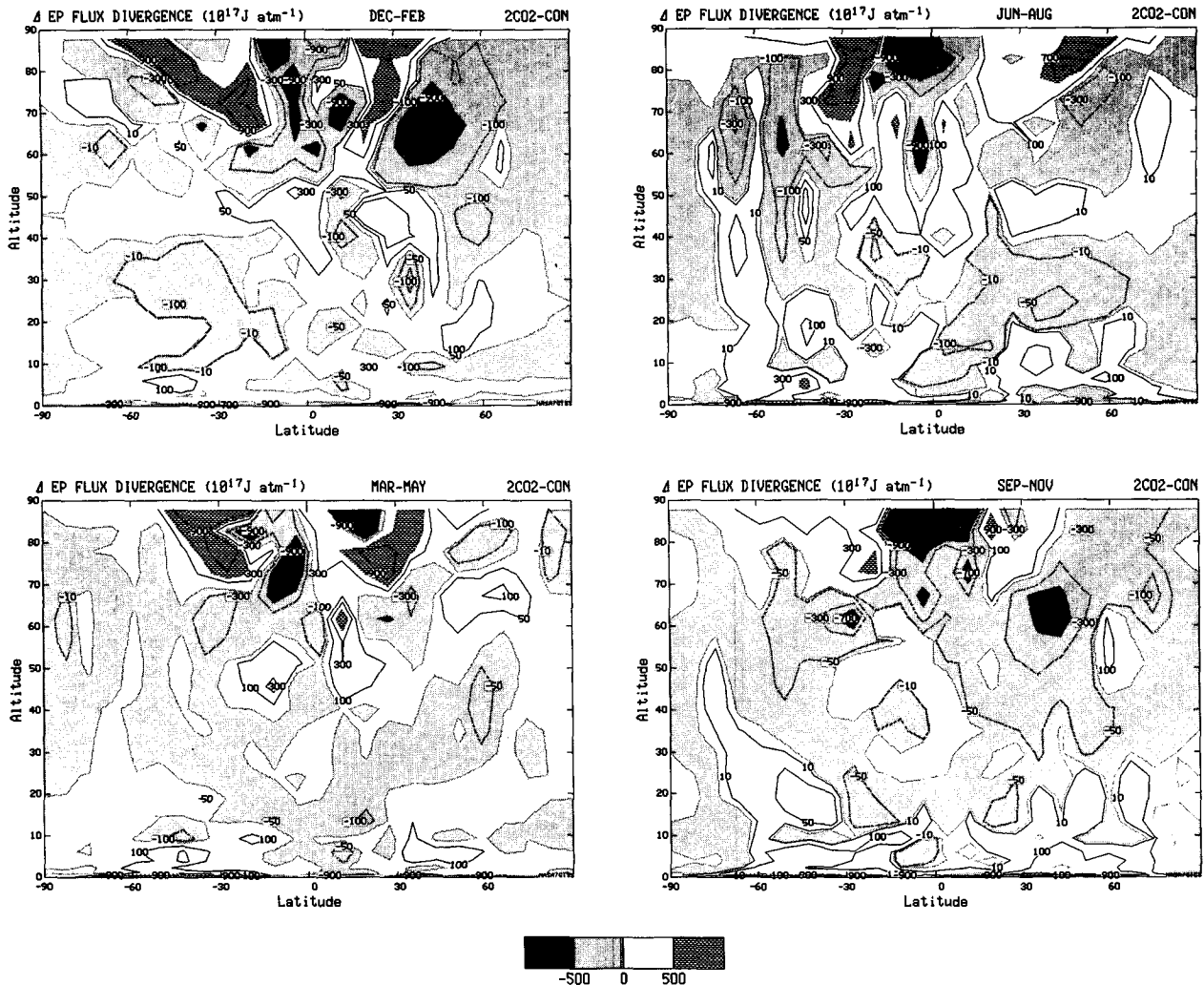


FIG. 8. Change of the Eliassen-Palm flux divergence in 2CO₂ for December-February (top left), March-May (bottom left), June-August (top right), and September-November (bottom right).

In fact, it proved impossible to examine the impact of radiative forcing alone, for in all three of these additional experiments the altered temperature and stability profiles affected tropospheric long wave generation and propagation. The return to December warmings therefore occurred in conjunction with eddy energy changes, regardless of stratospheric CO₂ levels. While the sample is too small to draw definitive conclusions, it would appear that the altered eddy energy propagation, characteristic of the full doubled CO₂ climate experiments, is the necessary component for changing the timing of the warmings.

4. Discussion

a. Dynamical considerations

The experiments described above divulged many interesting relationships, some of which were completely unexpected. The first, and foremost one is the

increased eddy energy in the middle atmosphere in all seasons. The expectation generated from the previous doubled CO₂ climate experiments was that eddy energy in the middle atmosphere would decrease, since decreases were clearly experienced in the troposphere, a result of reductions in the latitudinal temperature gradient. The middle atmosphere eddy energy increase was responsible for the increased residual circulation, and the dynamical warming of the polar winter stratopause.

Polar warming is not apparent in Fels et al. (1980) (for annual mean conditions and unaltered sea surface temperatures). The warming is apparent in the perpetual January simulation of Boville (1986), although it is weaker than in 2CO₂. As Boville's experiment also had unaltered sea surface temperatures, it is more comparable to ATM, and the warmings are indeed similar (Fig. 4, top). It is important to understand on what it depends, and whether it is model dependent.

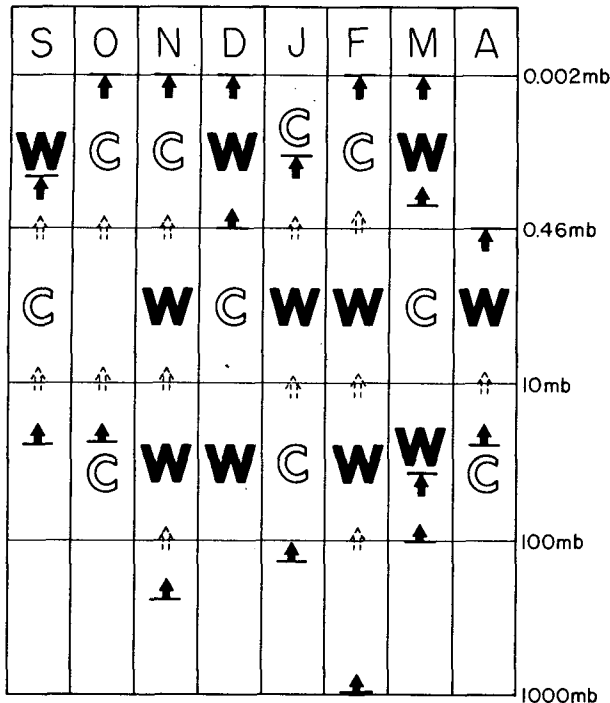


FIG. 9. Schematic of the relative change of temperature in the extratropics as a function of month during the extended winter season in the middle atmosphere, as summarized for 2CO₂, ALT and ATM, with W indicating warmer and C colder than the control run. Also shown are the beginning and ending levels for increases in the vertical EP flux, given by the dark arrows. The broken arrows indicate increased flux passed through the particular level.

The eddy energy increase is associated with the radiative temperature changes, warming in the troposphere and cooling in the stratosphere. The doubled CO₂ tropospheric warming varies somewhat from model to model, but are within the range of the various experiments performed here. The increased thermal cooling of the stratosphere is an expected result and will probably not vary greatly from model to model, although there is no proof that atmospheric radiative codes in different middle atmosphere models are exactly comparable. The temperature changes found by Fels et al. (1980) for the equatorial stratopause, and the values given by Boville (1987) are several degrees colder. It is not clear how directly applicable these other studies are, since they were performed with annual mean radiation (Fels et al. 1980) or perpetual January (Boville 1987) conditions; although the equatorial region is in approximate radiative equilibrium, dynamical temperature changes in these experiments in the equatorial stratopause region are on the order of several degrees per month (Fig. 3).

The combination of tropospheric warming and stratospheric cooling produces a relative destabilization of the atmosphere, which appears to affect the longest waves when sufficient vertical range is provided in the model. The doubled CO₂ potential energy increases for the tropospheric long waves in the GCMAM does

not occur in the 9-level climate model, possibly because the vertical destabilization is not as fully experienced in the limited vertical domain of the climate model (whose top is at 10 mb and which includes only one or two layers in the stratosphere). As indicated in Table 3, Northern Hemisphere kinetic energy in tropospheric waves 1–3 increases by some 5% in winter and spring in 2CO₂, while in the climate model this energy decreases by 5%. Although this difference is not large in percentage terms, it represents a great difference in the absolute amount of energy available for the stratosphere (since the troposphere has about 10 times more eddy energy than the lower stratosphere). This implies that an accurate depiction of tropospheric long wave changes may require a climate–middle atmosphere model.

The middle atmosphere eddy energy changes are also influenced by variations in the tropospheric wind structure/eddy energy propagation characteristics. This effect varies with the relative magnitude of the high latitude temperature amplification, as indicated by the differences between 2CO₂, ALT and ATM (Fig. 7). It will thus vary among the different modeling groups, which are presently getting different magnitudes of tropical/polar warming, at both the surface and in the upper troposphere.

Finally there is some evidence that in situ eddy energy generation in the stratosphere is favored by the vertical destabilization, whose average lapse rate decreases by some 25% on the annual average (from 1.4° km⁻¹ in the control run to 1.05° km⁻¹ in 2CO₂, between 13 and 51 km), along with the increased latitudinal temperature gradient in the lower stratosphere. Note the large percentage increases in summer in both hemispheres in Table 3, when tropospheric influence is minimized by stratospheric easterlies. If this result depends primarily on the radiative destabilization, it might well be simulated in all models run with doubled CO₂, given similarities in radiative schemes.

Once the eddy energy increases, the increased residual circulation and altered polar warmings become understandable phenomena. In the GCMAM, however, the residual circulation is also intensified by increased gravity wave drag in some of the experiments. In 2CO₂/ALT, increasing/decreasing tropospheric west winds tended to generate stronger/weaker mountain wave and shear wave sources, which then acted on the stronger/weaker stratospheric west winds. Convective sources generally increased in the warmer climate. While these results appear plausible, it must be emphasized that the highly nonlinear nature of the interaction between gravity waves and the atmospheric circulation make the actual gravity wave effect and its change very uncertain.

As discussed above in response to question 3, increased direct residual circulations in the stratosphere are associated with increased indirect circulations in the mesosphere. This change results in additional mesospheric cooling near the winter pole, and warming

over the summer pole. The magnitude of the mesospheric temperature changes, however, must be viewed with caution. The radiative response of the radiation code in the GCMAM to doubled CO_2 has been compared with that obtained from line-by-line calculations (Lacis, personal communication). The relative cooling shown by the model compares well with the calculated values up through 60 km; however, in the mesosphere, the model underestimates the cooling somewhat. This deficiency is at least partly offset by the spurious influence of the model top, which leads to vertical eddy heat flux divergences in the upper layers (1). With increased mesospheric eddy kinetic energy, especially in 2 CO_2 , the effect is amplified. An additional problem above 75 km is the possibility of nonlocal thermodynamic equilibrium, which cannot be handled by the radiation code, and insufficient numerical resolution, which affects radiation convergence values. Mesospheric results need to be evaluated with a more accurate radiation code and, ideally, with the top of the model located at higher levels.

The tropospheric response is also determined by the magnitude of the doubled CO_2 warming. Currently, the different GCMs are producing warming on the order of 4°–5°C, with 2 CO_2 and ALT having warming of 4.2°C. Wetherald and Manabe (1988) have emphasized the importance of upper troposphere cloud cover generation and vertical layering in influencing the magnitude of the warming. The GCMAM has different vertical layering in the troposphere, and allows cloud generation to occur at higher levels than in the standard 9-level climate model. Would it have produced the same amount of warming if run to equilibrium with doubled CO_2 ?

We can estimate the global warming characteristic of the GCMAM by noting that the difference in net radiation at the top of the atmosphere between 2 CO_2 and its control run for the three year average was close to 1 W m^{-2} coming into the atmosphere. This excess energy results from a greater increase in upper level clouds in the GCMAM, associated with its different vertical resolution, than occurred in the climate model from which the sea surface temperatures were derived. An initial imbalance in the doubled CO_2 run with the 9-level climate model of 4 W m^{-2} led to an ultimate warming of 4°C. We can expect that the energy imbalance in the GCMAM would have produced close to 1°C greater warming, for a total of about 5°C, as in the United Kingdom Meteorological Office model (Wilson et al. 1987). The greater warming would likely have amplified the effects shown here. Given that our knowledge of the true climate sensitivity is still somewhat uncertain, the expected response of the middle atmosphere to increased CO_2 , to the extent that it depends on tropospheric changes, will contain at least the same degree of uncertainty.

The arbitrary specification of the sea surface temperatures for all the experiments (except 2 CO_2) has another affect: it allows the land/ocean contrast to

change, which provides potential energy for long wave generation in the troposphere. The increased wave-number 2 energy in ALT is likely related to this phenomenon. It would be useful to rerun this experiment with a model that produces the greater high latitude amplification in a more natural fashion.

In addition to the possible impact of vertical resolution on model sensitivity, the delineation in the vertical of the equatorial tropopause will likely influence the water vapor changes predicted for the middle atmosphere. Control run temperatures are not quite cold enough at the equatorial tropopause, possibly because of insufficient vertical resolution to provide the thin layer in which the observed temperature minimum occurs. Thus the GCMAM control run had about twice the observed stratospheric water vapor after five years. 2 CO_2 shows an increase in stratospheric water vapor, on the order of about 0.5–1 ppmv, ATM shows a decrease, of 1–2 ppmv, and ALT has very small decreases. These values are consistent with the change in saturation mixing ratios associated with the changes in tropical lower stratosphere temperature in the different experiments, warming in 2 CO_2 of about 0.5°C, cooling in ATM of 1.5°C, with little change in ALT. Obviously, the degree of equatorial warming and convection which occurs in different models will influence this result. In addition, the concept of tropical “freeze-drying” of water vapor in the penetrative convective regions may involve highly complex physical processes, unlikely to be properly handled by the simple moist convective schemes included in current climate models. For this reason we did not allow the changes in water vapor predicted by the model to influence the radiation in the middle atmosphere; above 100 mb the control run and experiments used a constant value of 3 ppmv. Without greater understanding of tropospheric/stratospheric exchange of water vapor, and better parameterizations of tropical convection, modeled water vapor changes in the middle atmosphere must be labeled as highly speculative.

With CO_2 doubled in the troposphere and not in the stratosphere, the winter temperatures in the region from 200–50 mb (12–20 km) are often colder than with single or doubled CO_2 at all levels. The additional CO_2 in the troposphere, and the associated cloud and moisture increases, allow the upper troposphere to radiate more energy upward, and with reduced CO_2 in the stratosphere, less is absorbed and reradiated back down. The influence of this cooling in the model extends to the pressure level centered at 68 mb, even though CO_2 was not increased at this altitude.

Currently, CO_2 values do decrease with altitude from the troposphere to the stratosphere, although more gradually than that incorporated in these experiments, because CO_2 sources are located in the troposphere. As reported by Angell (1986), analysis of radiosonde data for the period 1960–1985 indicates a cooling of 0.5°C over that period in the upper troposphere and lower stratosphere. This is at variance with the climate

model simulation of Hansen et al. (1988), which incorporated uniform CO₂ changes with altitude, and produced an upper tropospheric warming. The upper tropospheric cooling in ATM-A and CO₂-A is thus qualitatively in the direction needed to align the model results with the observations (which are admittedly somewhat uncertain), and may emphasize the importance of differences between tropospheric and stratospheric CO₂ concentrations.

Potentially, changes in ozone would accompany changes in middle atmosphere temperature and dynamics. Cooler temperatures in the stratosphere would lead to decreased photochemical destruction, resulting in increased concentrations of ozone and increased solar ultraviolet heating, which could in turn offset some of the CO₂ cooling (e.g., Fels et al. 1980). On the other hand, increasing CO₂ will be taking place in a highly perturbed atmosphere (i.e., increased stratospheric chlorine, CH₄, NO₂, etc.), which in turn may lead to reduced levels of ozone. Reduced ozone levels in the Antarctic ozone "hole" may already be affecting the stratospheric circulation (Kiehl et al. 1988). The effect of both increased chlorine and lowered temperatures is to produce a more modified impact on ozone depletion (e.g., Connell and Wuebbles 1986). Ozone concentrations will be affected by future release rates of chlorofluorocarbons, and the proposed reduction in these sources would lead to more moderate ozone changes. If future ozone decreases are small, the assumption of no global ozone change, as used in all the experiments, becomes less of an issue, although doubled CO₂ experiments could well be run with specified changes in global ozone.

If the circulation of the stratosphere changes in intensity, however, it would undoubtedly lead to a redistribution of ozone. In particular, the doubled CO₂ experiments produce a more vigorous residual circulation; its possible effects on ozone and other trace gases are discussed below. Note that the Southern Hemisphere polar stratosphere cools substantially in all three experiments during spring. Shine (1987) has emphasized the importance of the ozone distribution for determining the temperature profile in this region. With a redistribution of ozone due to transport changes, the effect on the temperature in this region, and thus possibly ozone hole chemistry, might be very different. To fully resolve the effects of increased CO₂ on the middle atmosphere will require an interactive model that can accurately simulate stratospheric ozone, including the "hole."

b. Potential consequences of middle atmosphere changes

It is beyond the scope of this paper to explore in detail the implications of the doubled CO₂ stratospheric changes on atmospheric trace gases and chemistry. Nevertheless, some potential consequences can be discussed. Vertical advection and horizontal mixing in

the tropical stratosphere control both the distribution of stratospheric ozone and the atmospheric destruction rates for many trace gases. Perturbations to the stratospheric circulation, as shown here for the case of doubled CO₂, can lead more or less directly to changes in atmospheric composition and chemistry. The two most obvious changes in the stratosphere as a consequence of doubling CO₂ are the reduction in stratospheric temperatures and the increased net upward velocities in the tropical stratosphere.

Temperature changes are predicted to be as large as -10°C near the stratopause (50 km) and of order -4°C in the middle stratosphere (30 km). These results are similar to recent estimates of the temperature change from two-dimensional stratospheric chemical models (Eckman et al. 1987; Brasseur and Hitchman 1988). In these models the impact of doubled CO₂ occurs predominantly through the increased radiative cooling; the circulation and its changes cannot be calculated in a two-dimensional framework without making some assumptions about the eddy forcing of the stratosphere. Within the 2-D stratospheric models it has been demonstrated that the cooling of the lower stratosphere reduces the efficiency of ozone destruction, leading to an increase in the column abundance of ozone of 1%–4%. The present study confirms that temperature changes of this magnitude also result from the more complete GCM studies and are a consequence of the direct radiative cooling of the stratosphere. Therefore we support the primary conclusions from the chemical models that predict an increase in column ozone for a doubling of CO₂ alone.

Heterogeneous chemical reactions in the polar winter stratosphere depend critically on those regions of the stratosphere that become cold enough to form clouds. The interaction of gas-phase and aerosol chemistry is believed to be responsible for the formation of the Antarctic ozone "hole" and may play an important role in the recently detected trend in column ozone over northern midlatitudes in the late winter (NASA 1988). Predicted changes in temperatures in the Antarctic lower stratosphere (12–22 km) (Fig. 2) show that in winter the temperatures below 20 km may be warmer but during springtime all experiments show a cooling throughout the lower stratosphere. Thus, for the doubled-CO₂ atmosphere the chemical preconditioning during winter may be reduced, but the occurrence of polar stratospheric clouds should persist well into the spring.

The more vigorous stratospheric circulation in the doubled-CO₂ atmosphere is a result that could only be predicted with the use of a 3-D model. Its impact on the stratosphere is twofold: 1) increased global removal of N₂O and fully halogenated chlorofluorocarbons (CFCl₃, CF₂Cl₂, C₂F₃Cl₃, CF₃Br) and 2) a redistribution of ozone in the lower stratosphere from the tropics to the midlatitudes, reducing column ozone in the tropics.

Photolytic destruction within the stratosphere is the only significant loss for gases such as N_2O and the synthetic chlorofluorocarbons. The rate at which tropospheric air with relatively higher concentrations of these gases is delivered to the middle and upper stratosphere controls the globally integrated loss. We may expect the lifetimes of these long-lived gases (ranging currently from about 50 yr for $CFCl_3$ to about 150 yr for N_2O) to decrease inversely in proportion to the strength of the circulation. If the annual emissions of these gases were to remain constant, then their global concentrations would decline similarly in the doubled- CO_2 atmosphere.

The redistribution of column ozone may greatly affect tropospheric chemistry through the globally averaged destruction of trace gases by reaction with OH. Currently the tropical troposphere provides the major fraction of global loss for gases such as CO, CH_4 , CHF_2Cl and CH_3CCl_3 (see Logan et al. 1981). The concentration of tropospheric OH is highly sensitive to changes in the overhead ozone column; a reduction in column ozone of 4% would lead to equivalent increases in OH, and hence, in the loss rate for these gases. This projected change in column ozone for the tropics needs to be convolved with the other key atmospheric variables controlling tropospheric OH such as water vapor and cloud cover that are also likely to change in a doubled- CO_2 atmosphere (e.g., tropospheric water vapor increases by 11% in $2CO_2$).

A climatically perturbed atmosphere with more rapid advective transport via the residual circulation from the tropics to the midlatitudes may further accentuate the latitudinal gradient in the column abundance of ozone. On the other hand, if eddy energy also increases, then the downgradient eddy mixing of ozone between midlatitudes and the tropics may increase sufficiently to offset or even reverse this change in ozone gradient. At high latitudes, the increased residual circulation provides for greater downward transport into the troposphere, which might affect tropospheric ozone background values. The impact of this changed circulation on trace gases and ozone is currently being investigated using a 3-D chemical transport model with the GCM wind fields described here.

Finally, the occurrence of tropospheric warming and stratospheric cooling has the potential to change the altitude of the tropopause itself. The vertical level which delineates the change from warming below to cooling above at winter polar latitudes is lowest in ATM (~ 400 mb) and highest in ALT (~ 50 mb) (Figs. 1, 4). In the tropical regions, the level is lowest in ATM (~ 125 mb) and highest in $2CO_2$ (~ 60 mb). These differences are a direct consequence of the variation of input (sea surface) tropospheric heating in the different experiments. The actual change in tropopause altitude will depend upon how tropospheric heating and associated convective transport of heat to the upper troposphere really change as climate warms.

5. Concluding remarks

The primary results from these doubled- CO_2 experiments can be summarized as follows:

1) The stratosphere in general cools, while the troposphere warms. This leads to decreased vertical stability in the extratropical troposphere, which helps increase longwave generation in the troposphere, especially during Northern Hemisphere winter.

2) Increased tropical convection produces an increased latitudinal temperature gradient in the lower stratosphere. This leads to more in situ generation of eddy energy, as well as altering the atmospheric refractive properties to allow for better wave propagation conditions in some months.

3) Factors 1) and 2) increase the eddy energy in the middle atmosphere.

4) The increased eddy energy and eddy forcing drive a stronger residual circulation; additional influence in several of the experiments comes from greater gravity wave drag, associated with stronger tropospheric flow/shear/convection.

5) The pattern of eddy energy and propagation changes leads to an alteration of the typical stratospheric Northern Hemisphere winter pattern, with relative warming in November, January and February, and cooling in December and March.

6) The increased middle atmosphere eddy energy and residual circulation occur to some degree in all seasons, and in both hemispheres.

The doubled- CO_2 dynamical changes in the middle atmosphere are generally not large, often peaking at 10%–20% of the control run values, the same percentage change as occurs for tropospheric dynamical and hydrologic changes. The robustness of these changes is, however, suggested by the results from the series of experiments; many of the changes are on the order of two to three standard deviations at best, and thus of marginal statistical significance, again the same conclusion found for regional tropospheric dynamics and hydrology.

All the experiments were run with a coarse resolution model. To validate and improve the results, models need to be run with as fine resolution as is possible, which would at least help determine the possible resolution dependency of the tropospheric and stratospheric eddy energy changes. In addition, models will need to include interactive ozone calculations, which might alter features of the radiative response. Uncertainties in the tropospheric changes limit our confidence in some of the results, as illustrated by the differences among these experiments, and further uncertainties exist for changes in gravity wave effects. As was the case for doubled- CO_2 tropospheric climate changes, intercomparisons of doubled- CO_2 runs for the middle atmosphere are necessary to improve our understanding of model dependent processes and results.

Acknowledgments. We thank James Hansen for his generous support during the course of this work, Tristan Bukowski for computer graphics, and Lilly Del Valle and Jose Mendoza for help in preparation of the figures. This work was supported by the NASA Upper Atmosphere Program Office, while doubled carbon dioxide studies at GISS are supported by the United States Environmental Protection Agency.

REFERENCES

- Angell, J. K., 1986: Annual and seasonal global temperature changes in the troposphere and low stratosphere, 1960–1985. *Mon. Wea. Rev.*, **114**, 1922–1930.
- Arakawa, A., 1972: Design of the UCLA general circulation model. Tech Rep. No. 7, Dept. of Meteorology, University of California, Los Angeles, 116 pp.
- Boville, B., 1986: Detecting CO₂-induced temperature changes in the stratosphere. *Adv. Space Res.*, **6**, 45–50.
- Brasseur, G., and A. De Rudder, 1987: The potential impact on atmospheric ozone and temperature of increasing trace gas concentrations. *J. Geophys. Res.*, **92**, 10 903–10 920.
- , and M. Hitchman, 1988: Stratospheric response to trace gas perturbations: changes in ozone and temperature distributions. *Science*, **240**, 634–636.
- , A. De Rudder and C. Tricot, 1985: Stratospheric response to chemical perturbations. *J. Atmos. Chem.*, **3**, 261–288.
- Connell, P. S., and D. J. Wuebbles, 1986: Ozone perturbations in the LLNL one-dimensional model—Calculated effects of projected trends in CFCs, CH₄, CO₂, N₂O, and halons over 90 years. Report, Univer. of Calif. Radiat. Lab., Livermore, 1986.
- Eckman, R. S., J. D. Haigh and J. A. Pyle, 1987: An important uncertainty in coupled chlorine-carbon dioxide studies of atmospheric ozone modification. *Nature*, **329**, 616–619.
- Fels, S. B., 1985: Radiative-dynamical interactions in the middle atmosphere. *Advances in Geophysics*, **28**, 277–300.
- , J. D. Mahlman, M. D. Schwarzkopf and R. W. Sinclair, 1980: Stratospheric sensitivity to perturbations in ozone and carbon dioxide: radiative and dynamical response. *J. Atmos. Sci.*, **37**, 2265–2297.
- Hansen, J. E., G. Russell, D. Rind, P. Stone, A. Lacis, S. Lebedeff, R. Ruedy and L. Travis, 1983: Efficient three-dimensional global models for climate studies: models I and II. *Mon. Wea. Rev.*, **111**, 609–662.
- , A. Lacis, D. Rind, G. Russell, P. Stone, I. Fung, R. Ruedy and J. Lerner, 1984: Climate sensitivity: analysis of feedback mechanisms. *Climate Processes and Climate Sensitivity*, J. E. Hansen and T. Takahashi, Eds., American Geophysical Union, 130–163.
- , I. Fung, A. Lacis, D. Rind, S. Lebedeff, R. Ruedy, G. Russell and P. Stone, 1988: Global climate changes as forecast by Goddard Institute for Space Studies Three-Dimensional Model. *J. Geophys. Res.*, **93**, 9341–9364.
- Isaksen, I. S. A., and F. Stordal, 1986: Ozone perturbations by enhanced levels of CFCs, N₂O and CH₄: A two-dimensional diabatic circulation study including uncertainty estimates. *J. Geophys. Res.*, **91**, 5249–5263.
- Kiehl, J. T., 1986: Changes in the radiative balance of the atmosphere due to increases in CO₂ and trace gases. *Adv. Space Res.*, **6**, 55–62.
- , B. A. Boville and P. Briegleb, 1988: Response of a general circulation model to a prescribed Antarctic ozone hole. *Nature*, **332**, 501–504.
- Labitzke, K., B. Naujokat and J. K. Angell, 1986: Long-term temperature trends in the middle stratosphere of the Northern Hemisphere. *Adv. Space Res.*, **6**, 7–16.
- Leovy, C. B., C. R. Sun, M. H. Hitchman, E. E. Remsberg, J. M. Russell, L. L. Gordley, J. C. Gille and L. V. Lyjak, 1985: Transport of ozone in the middle atmosphere: evidence for planetary wave breaking. *J. Atmos. Sci.*, **42**, 230–244.
- Logan, J. A., M. J. Prather, S. C. Wofsy and M. B. McElroy, 1981: Tropospheric chemistry. *J. Geophys. Res.*, **86**, 7210–7254.
- Manabe, S., and R. T. Wetherald, 1975: The effects of doubling the CO₂ concentration on the climate of a general circulation model. *J. Atmos. Sci.*, **32**, 3–15, 1975.
- , and —, 1987: Large-scale changes of soil wetness induced by an increase in atmospheric carbon dioxide. *J. Atmos. Sci.*, **44**, 1211–1235.
- NASA, 1988: Present state of knowledge of the upper atmosphere 1988: An assessment report. R. T. Watson, M. J. Prather and M. J. Kurylo, Eds, NASA Ref. Pub. 1208, 200 pp.
- Ramanathan, V., R. J. Cicerone, H. B. Singh and J. T. Kiehl, 1985: Trace gas trends and their potential role in climate change. *J. Geophys. Res.*, **90**, 5547–5566.
- , L. Callis, R. Cess, J. Hansen, I. Isaksen, W. Kuhn, A. Lacis, F. Luther, J. Mahlman, R. Reck and M. Schlesinger, 1987: Climate-chemical interactions and effects of changing atmospheric trace gases. *Rev. Geophys.*, **25**, 1441–1482.
- Rind, D., 1986: The dynamics of warm and cold climates. *J. Atmos. Res.*, **43**, 3–24.
- , 1987: The doubled CO₂ climate: Impact of the sea surface temperature gradient. *J. Atmos. Sci.*, **44**, 3235–3268.
- , 1988a: The doubled CO₂ climate and the sensitivity of the modeled hydrologic cycle. *J. Geophys. Res.*, **93**, 5385–5412.
- , 1988b: Dependence of warm and cold climate depiction on climate model resolution. *J. Climate*, **1**, 965–997.
- , R. Suozzo, N. K. Balachandran, A. Lacis and G. Russell, 1988a: The GISS global climate/middle atmosphere model. Part I: model structure and climatology. *J. Atmos. Sci.*, **45**, 329–370.
- , —, and —, 1988b: The GISS global climate/middle atmosphere model. Part II: Model variability due to interactions between planetary waves, the mean circulation, and gravity wave drag. *J. Atmos. Sci.*, **45**, 371–386.
- Shine, K. P., 1987: The middle atmosphere in the absence of dynamical heat fluxes. *Quart. J. Roy. Meteor. Soc.*, **113**, 603–633.
- van Loon, H., R. A. Madden and R. L. Jenne, 1975: Oscillations in the winter stratosphere. *Mon. Wea. Rev.*, **103**, 154–162.
- Washington, W. M., and G. A. Miehle, 1984: Seasonal cycle experiment on the climate sensitivity due to a doubling of CO₂ with an atmospheric general circulation model coupled to a simple mixed-layer model. *J. Geophys. Res.*, **89**, 9475–9503.
- Wetherald, R. T., and S. Manabe, 1988: Cloud feedback processes in a general circulation model. *J. Atmos. Sci.*, **45**, 1397–1415.
- Wilson, C. A., J. F. B. Mitchell and W. M. Cunningham, 1987: A 2 × CO₂ climate sensitivity experiment with a global climate model including a sample ocean. Chapter 3, Final Report, Contract CL-114-UK(H), United Kingdom Meteorol. Office, Bracknell, United Kingdom.
- Wuebbles, D. J., F. M. Luther and J. E. Penner, 1983: Effect of coupled anthropogenic perturbations on stratospheric ozone. *J. Geophys. Res.*, **88**, 1444–1456.